OPEN ACCESS

Global Journal of Research in Engineering & Computer Sciences
ISSN: 2583-2727 (Online)
Volume 04| Issue 04 | July-Aug. | 2024
Journal homepage: https://gjrpublication.com/gjrecs/

Review Article

Adaptive Control of Quadrotor with Neural disturbance Estimator

Abdussamad Maaruf Fagge[1], Abubakar Surajo Imam[2], Lawal Mukhtar Ibrahim[3], Mukhtar Ibrahim Bello[4], *Muhammad Ahmad Baballe[5]

[1]National Space Research and Development Agency, Abuja, Nigeria.
[2,5]Department of Mechatronics Engineering, Nigerian Defence Academy Kaduna, Nigeria.
[3]Department of Electrical and Electronics Engineering, Altinbas University Istanbul, Turkey.
[4]Department of Computer Science, School of Technology, Kano State Polytechnic, Nigeria.

DOI: 10.5281/zenodo.13175683 **Submission Date: 10 June 2024 | Published Date: 03 Aug. 2024**

***Corresponding author: Muhammad Ahmad Baballe**
Department of Mechatronics Engineering, Nigerian Defence Academy Kaduna, Nigeria.
ORCID: 0000-0001-9441-7023

Abstract

Quadrotor UAVs are known to be affected by parametric uncertainties and external disturbances. These effects are addressed by designing efficient control methods for the fully-actuated and under-actuated subsystems of the quadrotor. A finite time fractional order sliding mode controller with integral error action (FISMC) is designed for the fully actuated subsystem to guarantee that all the states converged to the desired performances in short time. Moreover, a radial basis function neural network (RBFNN) is proposed to approximate the uncertain nonlinear function and the input gains. For the underactuated subsystem, a back-stepping fast-terminal sliding mode control (BFSMC) is developed to accomplished robust position tracking and produce the desired pitch and roll angles in finite time. Furthermore, a RBFNN is used to identify the lumped disturbances/uncertainties associated with the under-actuated subsystem without the knowledge of their bounds. With the aid of Lyapunov candidate function, the closed loop system has been guaranteed to converge to a small compact set in finite time. The efficacy of the proposed method is confirmed by comparing with other methods.

Keywords: RBFNN, finite time stability, fractional order, back-stepping, fast terminal sliding mode control.

I. INTRODUCTION

IN recent years, Unmanned Aerial Vehicles (UAVs) such as quadrotors are increasingly becoming an important part of scientific researches in academic, commercial, government, security and technological platforms [1]. The increasing popularity of quadrotors is due to their hovering capacity, low weight, low cost, maneuverability, small size, and vertical take-off & landing (VTOL) [2].

The dynamics of quadrotors are complex, nonlinear, underactuated multi-input-multi-output (MIMO), time varying, uncertain and affected by external disturbances. These make the control of quadrotors difficult and challenging. As a result, many researchers have come up with different control strategies to achieve stability and excellent tracking performances.

A nonsingular terminal SMC was proposed in [3] for trajectory tracking control of quadrotor taking into account the model uncertainties and external disturbances. In [4], a robust adaptive nonsingular fast terminal SMC was designed to control the attitude and the altitude of a quadrotor with parametric uncertainties and disturbances. In [5], an adaptive back-stepping fast terminal SMC was implemented for quadrotor attitude and position tracking control. An adaptive fractional SMC was implemented to take care of time varying load of a quadrotor [6]. A fractional order SMC has been designed for a quadrotor with constrained states [7]. A quadrotor controller has been constructed through fractional order SMC for a vision-based tracking of a moving vehicle [8]. In [9], a trajectory tracking controller based on fractional order SMC is presented for a quadrotor with time varying complex disturbances. A SMC was designed for a quadrotor with

time varying mass in order to achieve robust attitude tracking [10]. In [11], a SMC with modified super-twisting algorithm has been implemented for attitude control of 3 degree of freedom quadrotor. A sliding mode disturbance observer was designed for the suppression of external disturbances in [12], [13], [14]. The Coriolis terms and disturbances were estimated and compensated by the disturbance observer for aggressive maneuvering of quadrotor. A flight tracking controller based on disturbance observer has been suggested for a quadrotor and its effectiveness was validated by experiment [15]. In [16], a fault tolerant sliding mode disturbance observer was designed for a quadrotor subjected to actuator failure. An adaptive fault tolerant controller with disturbances observer has been applied to quadrotor in the presence of parametric uncertainties and external disturbances [17]. In [18], an adaptive state feedback fault tolerant controller is designed for a quadrotor with actuator failure. A sliding mode controller has been designed based on flat-quadrotor dynamics to solve the trajectory tracking issue of a quadrotor subjected to disturbances [19]. In [20], a novel robust proportional integral derivative (PID) controller was proposed for trajectory tracking of quadrotor and power reduction. A robust active disturbance rejection control has been presented in [21], [22] to control the attitude of a quadrotor. In [23], an active disturbance rejection control based on grey wolf optimization has been developed for quadrotor trajectory tracking. A double closed loop active disturbance rejection control has been designed in [24] to deal with complex nonlinearities, external disturbances and uncertainties. In [21], a composite active disturbance mitigation-based attitude controller was designed for a quadrotor under unknown disturbances. In [25], a robust back-stepping controller has been studied in order to control a quadrotor with time delay. A trajectory tracking controller for a quadrotor with slung load was presented in [26]. In [27], a nonlinear geometric control method was implemented in order to control a quadrotor with a point mass payload suspended by a string. In [28], a passivity-based control was designed to attenuate the swing angle of slung load transported by a quadrotor.

The model of a quadrotor was identified in [29] and a robust H_∞ attitude controller was developed to guarantee tracking performance and disturbance rejection. A sigmoid tracking differentiator together with robust back-stepping controller was used to obtain the tracking control of a quadrotor under external disturbances [30]. A fast terminal SMC with integral error has been used to solve flight problems of quadrotor UAV with varying uncertainties [31]. An adaptive back-stepping control based on state observer has been studied in [32] for path tracking of a quadrotor. In [33], a back-stepping method was combined with SMC to control the orientation and the displacement of a quadrotor in the presence of unknown uncertainties. Extended state observer is combined with backstepping based SMC in order control a small size UAV [34].

The universal approximation property of NN and fuzzy logic systems (FLS) result in their wider applications in adaptive control [35]. In [1], a NN was used to tune the parameters of SMC for each subsystem of a quadrotor. A robust neuroadaptive controller has been implemented for a quadrotor to track moving objects [36]. In [37], a RBFNNs together with proportional-derivative SMC was proposed to control the position subsystem of a quadrotor. In [38], an adaptive RBFNN SMC is used to dealt with uncertain nonlinearities and achieve robust trajectory tracking of the quadrotor. In [39], a quadrotor with actuator faults was investigated and RBFNN based SMC fault tolerant controller was developed to guarantee that the states converge to the required responses. In [40], a Fuzzy based attitude controller was developed for the hovering control of a quadrotor. In [41], a type-2 fuzzy dynamic surface control of multiple quadrotors has been studied. The unmodelled dynamics of a quadrotor have been identified based on NN and a back-stepping controller was employed for trajectory tracking [42]. An adaptive RBFNN integral SMC is applied to control the position of a quadrotor with uncertainties [43].

A faster convergence, quick recovery from external disturbances, and excellent tracking performance can be obtained by finite time control schemes. a finite time ADRC has been designed for attitude tracking of quadrotor under input-saturation [44]. A finite time hybrid controller has been designed for accurate trajectory tracking of quadrotor [45]. An adaptive multivariable controller based on finite time stability has been proposed for attitude control of quadrotor with external disturbances [46]. A finite time-based integral SMC has been designed for a quadrotor with parametric uncertainties [47].

Inspired by the aforesaid discussion, a finite time control schemes are proposed to track the attitude and position of a quadrotor in the presence of parametric uncertainties and external disturbances. A RBFNN based fractional order integral SMC (NN-FISMC) is designed for the finite time control of the fully-actuated subsystem. Moreover, a backstepping based fast terminal SMC with neural disturbance estimator (NN-BFSMC) is developed for the tracking of the under-actuated subsystem (position subsystem) and generate the desired signals. The main contributions of this paper are summarized as follows:

1. The finite time control scheme is employed to ensure faster convergence and trajectory tracking.
2. The NN-FISMC is proposed to improve the robustness of the control system to uncertainties and external disturbances. Contrary to the fractional order SMC in [7], [6], [8], [9], the NN-FISMC in this paper has integral error term to eliminate the steady state error, finite time convergence to the reference signals and completely independent of the system dynamics.

3. In [37], [38], [42], [43], [43], [39], a RBFNN was employed to approximate only the uncertain nonlinear functions while input gains were assumed to be free from uncertainties. This reduced extra complications in the control design. However, in practical applications, the assumption can lead to inaccurate control. In this work, both the uncertain nonlinear functions and the input gains of the quadrotor fully-actuated subsystem are estimated by RBFNN in order ensure robust performances.
4. In [47], 13 adaptation laws have been used to estimate all the uncertain parameters of the fully-actuated subsystem of the quadrotor. In this paper, 8 RBFNNs are used to estimate the 4 uncertain nonlinear functions and the four input gains of the quadrotor fully-actuated subsystem. Hence, the number of computations is reduced.
5. In [45], a back-stepping method was developed to control the horizontal position subsystem of a quadrotor. In [48], an improved control action was achieved by combining back-stepping, fast terminal SMC, and an adaptive law which estimate the upper bounds of the external disturbances. Nevertheless, the adaptive estimation is more effective for constant disturbances. In this work, a NN-BFTSMC is proposed to stabilized the position subsystem in short time. The RBFNN can accurately approximate any complex time varying disturbances unlike the adaptive methods.

The rest of the paper is arranged as follows: The mathematical model is given in Section II. The finite time controller is designed in Section III. The simulation results are presented in Section IV. In Section V, the conclusions are drawn.

II. DYNAMIC MODELLING

This paper considers a rigid cross-frame and symmetric quadrotor subjected to aerodynamic drag, parametric uncertainties and wind gust. The six degrees of freedom of the quadrotor is determined by the body fixed frame whose origin coincides with the center of gravity of the quadrotor and the fixed earth frame. The position of the center of gravity is represented by the vector $\zeta = [x, y, z]$ in the fixed earth frame, while the attitude of the quadrotor is represented by $\eta = [\phi, \theta, \psi]$ where ϕ is the roll angle, θ is the pitch angle, and ψ is the yaw angle. The dynamic equations of the quadrotor can be expressed in Newton-Euler form as [49]:

$$\ddot{\phi} = \frac{1}{I_x}\left[-K_\phi \dot{\phi}^2 + (I_y - I_z)\dot{\psi}\dot{\theta} - J_r\omega_r\dot{\theta}\right] + \frac{lu_2}{I_x} + \delta_\phi \quad (1)$$

$$\ddot{\theta} = \frac{1}{I_y}\left[-K_\theta \dot{\theta}^2 + (I_z - I_x)\dot{\psi}\dot{\phi} + J_r\omega_r\dot{\theta}\right] + \frac{l}{I_y u_3} + \delta_\theta \quad (2)$$

$$\ddot{\psi} = \frac{1}{I_x}\left[-K_\psi \dot{\psi}^2 + (I_x - I_y)\dot{\phi}\dot{\theta}\right] + \frac{l}{I_z}u_4 + \delta_\phi \quad (3)$$

$$\ddot{z} = -\frac{K_z}{m}\dot{z} - g + \frac{1}{m}(\cos\phi\cos\theta)u_1 + \delta_z \quad (4)$$

$$\ddot{y} = -\frac{K_y}{m}\dot{y} + (\cos\phi\sin\theta\sin\psi + \sin\phi\cos\psi)\frac{u_1}{m} + \delta_y \quad (5)$$

$$\ddot{x} = -\frac{K_x}{m}\dot{x} + (\cos\phi\sin\theta\cos\psi + \sin\phi\sin\psi)\frac{u_1}{m} + \delta_x \quad (6)$$

where m is the mass of the quadrotor, g is the acceleration due to gravity, I_x, I_y, I_z are the inertias, $K_x, K_y, K_z, K_\phi, K_\theta$ and K_ψ are the drag coefficients, $\delta_\phi, \delta_\theta, \delta_\psi, \delta_x, \delta_y, \delta_z$ denote the external disturbances, parametric uncertainties and unmodeled dynamics, $\omega_r = (\omega_4 + \omega_4 - \omega_2 - \omega_1)$ is the quadrotor relative speed, $\omega_1 - \omega_4$ are the rotor speeds related by

$$\begin{bmatrix} u_1 \\ u_2 \\ u_3 \\ u_4 \end{bmatrix} = \begin{bmatrix} K_p & K_p & K_p & K_p \\ -K_p & 0 & -K_p & 0 \\ 0 & -K_p & 0 & -K_p \\ C_d & C_d & C_d & C_d \end{bmatrix} \begin{bmatrix} \omega_1^2 \\ \omega_2^2 \\ \omega_3^2 \\ \omega_4^2 \end{bmatrix}$$

u_1 is the altitude control signal, u_2, u_3 and u_4 are the roll, pitch and yaw inputs respectively, K_p and C_d are the aerodynamic force and moment coefficients respectively.

The fully actuated subsystem of the quadrotor is extracted from (1)-(6) as

$$\begin{cases} \Upsilon_1 = \Upsilon_2 \\ \Upsilon_2 = f_\Upsilon + b_\Upsilon u + \delta_\Upsilon \end{cases} \quad (7)$$

where $\Upsilon_1 = [\phi \quad \theta \quad \psi]^T, \Upsilon_2 = [\dot{\phi} \quad \dot{\theta} \quad \dot{\psi}]^T, \delta_\Upsilon = [\delta_\phi \quad \delta_\theta \quad \delta_\psi]^T, u = [u_2 \quad u_3 \quad u_4]^T$

$$f_Y = \begin{bmatrix} \frac{1}{I_x}\left[-K_{a\phi}\dot{\phi}^2 + (I_y - I_z)\dot{\psi}\dot{\theta}^2 - J_r\Omega_r\dot{\theta}\right] \\ \frac{1}{I_y}\left[-K_{a\theta}\dot{\theta}^2 + (I_z - I_x)\dot{\psi}\dot{\phi} + J_r\Omega_r\dot{\theta}\right] \\ \frac{1}{I_x}\left[-K_{a\psi}\dot{\psi}^2 + (I_x - I_y)\dot{\phi}\dot{\theta}\right] \end{bmatrix}$$

$$b_Y = \begin{bmatrix} \frac{l}{I_x} & 0 & 0 \\ 0 & \frac{l}{I_y} & 0 \\ 0 & 0 & \frac{l}{I_z} \end{bmatrix}$$

The under-actuated subsystem is given by

$$\begin{cases} \Omega_1 = \Omega_2 \\ \Omega_2 = f_\Omega + b_\Omega v + \delta_\Omega \end{cases} \tag{8}$$

where $\Omega_1 = [z \quad y \quad x]^T, \Omega_2 = [\dot{z} \quad \dot{y} \quad \dot{x}]^T, \delta_\Omega = [\delta_z \quad \delta_y \quad \delta_x]^T, v = [u_1 \quad u_y \quad u_x]^T$

$$\begin{bmatrix} u_x \\ u_y \end{bmatrix} = \begin{bmatrix} (\cos\phi \sin\theta \cos\psi + \sin\phi \sin\psi) \\ (\cos\phi \sin\theta \sin\psi - \sin\phi \cos\psi) \end{bmatrix}$$

$$f_\Omega = \begin{bmatrix} \frac{K_{ax}}{m}\dot{x} \\ \frac{K_{ay}}{m}\dot{y} \\ \frac{K_{az}}{m}\dot{z} - g \end{bmatrix}; b_\Omega = \begin{bmatrix} \frac{(\cos\phi \cos\theta)}{m} & 0 & 0 \\ 0 & u_1/m & 0 \\ 0 & 0 & u_1/m \end{bmatrix}$$

Then, the desired pitch and roll angles can be obtained as

$$\begin{cases} \phi_d = \arcsin\left(u_x \sin\psi - u_y \cos\psi\right) \\ \theta_d = \arcsin\left(\frac{u_x \cos\psi + u_y \sin\psi}{\cos\phi_d}\right) \end{cases} \tag{9}$$

III. CONTROL DESIGN

In this section, a RBFNN based finite time controllers are designed for the quadrotor subjected to external disturbances and model uncertainties to track the reference trajectories. The aim is to derive the state variables $[\phi\theta\psi zyx]^T$ to follow the desired state values $[\phi_d \quad \theta_d \quad \psi_d \quad z_d \quad y_d \quad x_d]^T$. The control architecture is shown in Fig. 1.

Lemma 1: [50] For any real number $a > 0, b > 0$ if there exists a continuous positive definite function meeting the inequality,

$$\dot{L} \leq -aL^m + b \tag{10}$$

the equilibrium point is semi-globally finite time stable

Definition 1: [51] The definition of fractional order derivatives according to Caputo is given by

$$D_t^\sigma f(t) = \frac{1}{\Gamma(n-\sigma)} \int_0^t \frac{f^n(\tau)}{(t-\tau)^{\sigma-n+1}} d\tau \tag{11}$$

where n is an integer so that $n-1<\sigma<n$ and $\Gamma(.)isa$ Gamma function
Assumption 1: The disturbances $\delta_i(i=\phi\theta\psi zyx)$ are continuously differentiable and uniformly bounded by unknown bounds δ_{bi}

$$\delta_i \leq \delta_{bi} \tag{12}$$

Assumption 2: The desired values $[\phi_d\theta_d\psi_d z_d y_d x_d]^T$ are Lipschitz continuous.

A. RBFNN Approximation

RBFNN can approximate any continuous nonlinear function in a small compact set. The RBFNN has a simple structure and does not need complex calculations. In addition, it has a superior generalization capability than the multiple layers neural network.

The RBFNN consists of three layers: the input, the hidden and the output layers. The hidden layer activation function is usually a Gaussian function expressed as

$$\zeta_j(X_i)=\exp\left(-\frac{\|X_i-c_j\|^2}{\gamma_j}\right) \tag{13}$$

where $X_i\in R^n$ is the input vector, γ_j is the width of the Gaussian function, c_j is the center of the receptive field. If there exist an optimal weight vector, W, and $P(X_i)$ is the RBFNN output, then

$$P(X_i)=V^T\zeta(X_i)+\varepsilon_P \tag{14}$$

$$\varepsilon_P\leq\varepsilon_P^* \tag{15}$$

where ε_P is the approximation error satisfying $\varepsilon_P\leq\varepsilon_P^*$, with ε_P^* being the maximum of the RBFNN approximation error.

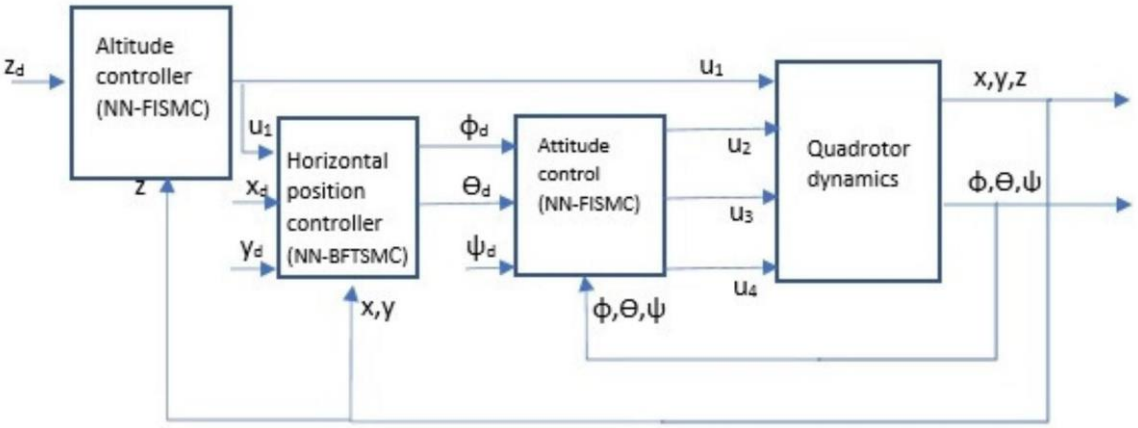

Fig. 1. Control architecture

B. NN-FISMC controller design

The aim of this section is to design the controller v for the underactuated subsystem to guarantee the attitude tracking error e_Υ converges to zero asymptotically.

Let $\Upsilon_d=[\phi_d\quad\theta_d\quad\psi_d]^T$ be the desired attitude trajectory. The attitude tracking errors are thus

$$e_\Upsilon=\Upsilon_1-\Upsilon_d;\ \dot{e}_\Upsilon=\dot{\Upsilon}_1-\dot{\Upsilon}_d;\ \ddot{e}_\Upsilon=\dot{\Upsilon}_2-\ddot{\Upsilon}_d$$

The fractional order sliding mode surfaces is given by:

$$S=\dot{e}_\Upsilon+\lambda\int_{t_0}^{T_f}e_\Upsilon dt+\Lambda D^{\sigma-1}e_\Upsilon \tag{16}$$

Using the RBFNN to approximate $f_\Upsilon + \delta_\Upsilon$, the time derivatives of the surface is

$$\dot{S} = \ddot{\Upsilon} - \ddot{\Upsilon}_d + \lambda \dot{e}_\Upsilon + \Lambda D^\sigma e_\Upsilon \tag{17}$$

The error trajectories reached the sliding surfaces based on $S = \dot{S} = 0$ and the reaching law chosen in this study is

$$u_r = -\eta S \ \in \mathcal{R}^{3\times 1} \tag{18}$$

where $\lambda \in \mathcal{R}^{3\times 3} > 0, \Lambda \in \mathcal{R}^{3\times 3} > 0, \eta \in \mathcal{R}^{3\times 3} > 0$ are design diagonal matrices. The control inputs for the entire four degree of freedom required to reach and stay on the respective sliding surfaces in finite time are:

$$u = \hat{g}(x)^{-1}\left[-\hat{F}(x) + \ddot{\Upsilon}_d - \lambda \dot{e} - \Lambda D^\sigma e - \eta S\right] \tag{19}$$

where $\hat{F}$ and $\hat{g}$ are the estimates of the unknown functions F and g respectively.
Remark 1: When $\hat{g} \longrightarrow 0$, the control law (19) is undefined. Therefore, we assume $|\hat{g}| \geq q > 0$. where q is a small known lower bound to keep $\hat{g}(x)$ away from zero [52].
Adding $(\hat{g}(x)u - \hat{g}(x)u)$ and substituting (19) into (17) yield

$$\begin{aligned} \dot{S} = F(x) + \frac{\hat{g}(x)}{\hat{g}(x)^{-1}}\left[-\hat{F}(x) + \ddot{\Upsilon}_d - \lambda \dot{e} - \Lambda D^\sigma e - \eta S\right] \\ +[g(x) - \hat{g}(x)]u - \ddot{\Upsilon}_d + \lambda \dot{e} + \Lambda D^\sigma e \end{aligned} \tag{20}$$

$$V = \begin{bmatrix} V_z^\top \\ V_\phi^\top \\ V_\theta^\top \\ V_\psi^\top \end{bmatrix}; W = \begin{bmatrix} W_z^T & 0 & 0 & 0 \\ 0 & W_\phi^T & 0 & 0 \\ 0 & 0 & W_\theta^T & 0 \\ 0 & 0 & 0 & W_\psi^T \end{bmatrix}$$

$$\zeta(X_i) = \begin{bmatrix} \zeta_z & 0 & 0 & 0 \\ 0 & \zeta_\phi & 0 & 0 \\ 0 & 0 & \zeta_\theta & 0 \\ 0 & 0 & 0 & \zeta_\psi \end{bmatrix}; \varepsilon_f = \begin{bmatrix} \varepsilon_{f_z} \\ \varepsilon_{f_\phi} \\ \varepsilon_{f_\theta} \\ \varepsilon_{f_\psi} \end{bmatrix}$$

$$\varepsilon_g = \begin{bmatrix} \varepsilon_{g_z} & 0 & 0 & 0 \\ 0 & \varepsilon_{g_\phi} & 0 & 0 \\ 0 & 0 & \varepsilon_{g_\theta} & 0 \\ 0 & 0 & 0 & \varepsilon_{g_\psi} \end{bmatrix}$$

The adaptive RBFNN is

$$\hat{F}(X_i) = \hat{V}^T \zeta(X_i) \tag{21}$$

$$\hat{g}(X_i) = \hat{W}^T \zeta(X_i) \tag{22}$$

The RBFNN function estimation errors are as follows:

$$\tilde{F}(X_i) = \tilde{V}^T \zeta(X_i) + \varepsilon_f \tag{23}$$

$$\tilde{g}(X_i) = \tilde{W}^T \zeta(X_i) + \varepsilon_g \tag{24}$$

where $\tilde{V} = V - \hat{V}$ and $\tilde{W} = W - \hat{W}$ are RBFNN estimation errors. Substituting (23) and (24) into (17) gives

$$\dot{S} = \tilde{V}^T \zeta(X_i) + \varepsilon_f + \left[\tilde{W}^T \zeta(X_i) + \varepsilon_g\right]u - \eta S \tag{25}$$

Theorem 2: Consider the open-loop system (1)-(6), the control input (19), with NN estimation algorithms given as

$$\begin{cases} \dot{\hat{V}} = S^T \xi_1 \zeta(X) - \mu \xi_1 \hat{V} \\ \dot{\hat{W}} = S^T \xi_2 \zeta(X) u - \mu \xi_2 \hat{W} \end{cases} \tag{26}$$

where $\xi_1 = \xi_1^T > 0 \in \mathcal{R}^{3\times3}, \xi_2 = \xi_2^T > 0 \in \mathcal{R}^{3\times3}$ are tuning matrices, $\mu > 0$ is a small constant. Therefore, $S, \tilde{V}$, and $\tilde{W}$ are ultimately uniformly semi-globally bounded in finite time near the compact set $\Omega_{q_1} \equiv \{q_1: \|q_1\| \leq c_{q_1}\}$, where $c_{q_1} > 0$ is a small constant.

Proof 1: To begin with, the Lyapunov function candidate is chosen as

$$L_1 = \frac{1}{2}S^TS + \frac{1}{2}\tilde{V}^T\xi_1^{-1}\tilde{V} + \frac{1}{2}\tilde{W}^T\xi_2^{-1}\tilde{W} \tag{27}$$

Differentiating (27) with respect to time and substituting $\dot{V} = \dot{W} = 0$, we have

$$\dot{L}_1 = S^T\dot{S} - \tilde{V}^T\xi_1^{-1}\dot{\hat{V}} - \tilde{W}^T\xi_2^{-1}\dot{\hat{W}} \tag{28}$$

Substituting the adaptation algorithms (26) into (28), one has

$$\dot{L}_1 = -S^T\eta S + \mu\tilde{V}^T\hat{V} + \mu\tilde{W}^T\hat{W} + S^T\epsilon_F + S^T\epsilon_g u \tag{29}$$

Consider the following Young's inequalities

$$\begin{cases} S^T\epsilon_F \leq \dfrac{\| S \|^2}{2} + \dfrac{\|\epsilon_F\|^2}{2};\ S^T\epsilon_g u \leq \dfrac{\| S \|^2}{2} + \dfrac{\|\epsilon_g u\|^2}{2} \\ \mu\tilde{V}^T\hat{V} = \mu\tilde{V}^T[V - \tilde{V}] \leq \mu\dfrac{\| V \|^2}{2} - \mu\dfrac{\| \tilde{V} \|^2}{2} \\ \mu\tilde{W}^T\hat{W} = \mu\tilde{W}^T[W - \tilde{W}] \leq \mu\dfrac{\| W \|^2}{2} - \mu\dfrac{\| \tilde{W} \|^2}{2} \end{cases}$$

Substituting the inequalities into (26), we get

$$\begin{aligned} \dot{L}_1 \leq -a_1\left[\tfrac{1}{2}\| S \|^2 + \tfrac{1}{2}\xi_{1min}^{-1}\| \tilde{V} \|^2 + \tfrac{1}{2}\xi_{2min}^{-1}\| \tilde{W} \|^2\right] \\ +\mu\tfrac{\|W\|^2}{2} + \mu\tfrac{\|V\|^2}{2} + \tfrac{\|\epsilon_F\|^2}{2} + \tfrac{\|\epsilon_g u\|^2}{2} \end{aligned} \tag{30}$$

where $a_1 = \min\{(2\eta_{\min} - 1), \mu\xi_{1\min}, \mu\xi_{2\min}\}$, $b_1 = \mu\frac{\|W\|^2}{2} + \mu\frac{\|V\|^2}{2} + \frac{\|\epsilon_F\|^2}{2} + \frac{\|\epsilon_g u\|^2}{2}$, $\eta_{\min}$, $\xi_{1\,\min}$, and $\xi_{2\,\min}$ are the minimum Eigen values of η, ξ_1, and ξ_2 respectively. Multiplying both sides of (30) by $e^{a_1 t}$ and integrating the resulting equation produces

$$L_1 \leq \left(L_1(0) - \frac{b_1}{a_1}\right)e^{-a_1 t} + \frac{b_1}{a_1} \leq L_1(0) - \frac{b_1}{a_1} \tag{31}$$

Taking into account the Lyapunov function (27), one can gets

$$\frac{1}{2}\|q_1\|^2 \leq L(0) - \frac{b_1}{a_1} \Rightarrow \|q_1\| \leq \sqrt{2\left(L(0) - \frac{b_1}{a_1}\right)} \tag{32}$$

In view of (32), all the closed-loop signals $S, \tilde{W}$ and $\tilde{V}$ are uniformly ultimately semi-global bounded in a compact set defined by $\Omega_{q_1} \equiv \{q_1: \|q_1\| \leq c_{q_1}\}$. where $c_{q_1} \equiv \sqrt{(L(0) - \kappa_2/\kappa_1)}\forall t \leq t_0 + T_1$, and T_1 is the finite settling time.

C. NN-BFTSMC for under-actuated subsystem

In this section, the state space model of the under-actuated subsystem is represented in terms of the known nominal and the uncertain parts (33). The uncertain part is approximated by RBFNN.

$$\begin{cases} \dot{M} &= N \\ \dot{N} &= f_2 + g_2 u_{xy} + \delta_2 \end{cases}$$

where

The lumped uncertainties/disturbances can be approximated by a RBFNN as $\delta_2 = W^{*T}\beta(X_i) + \epsilon_{\delta_2}$. The RBFNN estimate of δ_2 is as follows

$$\hat{\delta}_2 = \hat{W}^{*T}\beta(X_i) \tag{33}$$

were

$$W^* = \begin{bmatrix} W_x^{*\top} \\ W_y^{*\top} \end{bmatrix}; \beta = \begin{bmatrix} \zeta_x(X_i) & 0 \\ 0 & \zeta_y(X_i) \end{bmatrix}; \epsilon_{\delta_2} = \begin{bmatrix} \epsilon_{\delta_x} \\ \epsilon_{\delta_y} \end{bmatrix}$$

and the RBFNN estimation error is

$$\tilde{\delta}_2 = \delta_2 - \hat{\delta}_2 = \tilde{W}^{*T}\beta(X_i) + \epsilon_{\delta_2} \tag{34}$$

Let $\varrho = M - M_d$ be the tracking error. The fast-terminal sliding mode surfaces are given as

$$S = \dot{\varrho} + c\varrho + h\varrho^{p/q} \tag{35}$$

where $c \in \mathcal{R}^{2\times2}$ and $h \in \mathcal{R}^{2\times2}$ are constant diagonal matrices, $q > p > 0$ are design parameters. Differentiating (35) with respect to time yields

$$\dot{S} = \ddot{\varrho} + c\dot{\varrho} + \frac{p}{q}h\text{diag}\,(\dot{\varrho})\varrho^{p/q-1} \tag{36}$$

Substituting (33) into (35) yields

$$\dot{S} = f_2 + g_2u_{xy} + \delta_2 - \ddot{M}\ddot{d}_d + c\dot{\varrho} + h\frac{p}{q}\text{diag}\,(\dot{\varrho})\varrho^{p/q-1} \tag{37}$$

Remark 2: The term $\varrho^{p/q-1} \longrightarrow \infty$ when $\varrho = 0$. This singularity is avoided by modifying the sliding mode surface as [53] $S = \dot{\varrho} + c\varrho + h\Phi(\varrho)$. The function $\Phi(\varrho)$ is given by

$$\Phi(\varrho) = \begin{cases} \varrho^{p/q}, & \text{if } \bar{S} = 0 \text{ or } \bar{S} \neq 0 |\varrho| > \tau \\ \varrho, & \text{if } \bar{S} \neq 0, |\varrho| \leq \tau \end{cases}$$

where $\bar{S} = \dot{\varrho} + c\varrho + h\varrho^{p/q}, \tau$ denote a small constant threshold.

Define the following Lyapunov function and its derivative as

$$L_2 = \frac{1}{2}\varrho^T\varrho \tag{38}$$

$$\dot{L}_2 = \varrho^T(N - \dot{M}_d) \tag{39}$$

If the virtual input is designed as $N = S - c\varrho + \dot{M}$, we have

$$\dot{L}_2 = -\varrho^T c\varrho + S^T\varrho \tag{40}$$

Consider the following new Lyapunov function

$$L_3 = \frac{1}{2}\varrho^T\varrho + \frac{1}{2}S^TS + \frac{1}{2}\tilde{W}^{*T}\xi_3^{-1}\tilde{W}^* \tag{41}$$

Differentiating (41) with respect to time gives

$$\begin{aligned} \dot{L}_3 &= \varrho^T\dot{\varrho} + S^TS + \tilde{W}^{*T}\xi_3^{-1}\dot{\tilde{W}}^* \\ &= -\varrho^Tc\varrho + S^T\big(f_2 + g_2u_{xy} + W^{*T}\beta(X_i) + \epsilon_{\delta_2} \\ &\quad -\ddot{M}_d + \varrho + c\dot{\varrho} + \frac{p}{q}k\text{diag}\,(\dot{e})e^{p/q-1}\big) \end{aligned} \tag{42}$$

The control input and the RBFNN weight update law are designed as

$$u_{xy} = g^{-1}\big(-f - \hat{W}^{*T}\beta(X_i) + \ddot{M}_d - \varrho - c\dot{\varrho} \tag{43}$$

$$\xi_3 = \xi_3^T > 0 \in \mathcal{R}^{2\times2} \tag{44}$$

where $\xi_3 = \xi_3^T > 0 \in \mathcal{R}^{2\times2}$ is a constant diagonal matrix and $\mu > 0$ is a small constant. Substituting (43) (42) gives

$$\dot{L}_3 = -\varrho^Tc\varrho - S^TKS + S^T\epsilon_{\delta_2} + \mu\tilde{W}^{*T}\dot{\hat{W}}^* \tag{45}$$

Consider the following inequalities

$$\begin{cases} S^T\epsilon_D \le \dfrac{\| S \|^2}{2} + \dfrac{\|\epsilon_D\|^2}{2} \\ \tilde{W}^{*T}\hat{W}^* = \tilde{W}^{*T}\left[W^* - \tilde{W}^*\right] \le \dfrac{\|W^*\|^2}{2} - \dfrac{\|\tilde{W}^*\|^2}{2} \end{cases}$$

Substituting the inequalities into (45) gives

$$\begin{aligned} \dot{L}_3 \le -a_2\left[\frac{\|\varrho\|^2}{2} + \frac{\|S\|^2}{2} + \frac{\xi_{3\min}^{-1}\|\tilde{W}^*\|^2}{2}\right] \\ +\mu\frac{\|W^*\|^2}{2} + \frac{\|\epsilon_D\|^2}{2} \end{aligned} \tag{46}$$

where $a_2 = \min\{2\lambda_{2\min}, (2k_{\min} - 1), \mu\xi_{3\min}\}$, $b_2 = \frac{\|W^*\|^2}{2} + \frac{\|\epsilon_D\|^2}{2}$.

Multiplying both sides of (46) by $e^{a_2 t}$ and integrating the resulting equation, we get

$$\|q_2\| \le \sqrt{2\left(L_2(0) - \frac{b_2}{a_2}\right)} \equiv c_{q_2} \tag{47}$$

Hence, all the closed-loop signals e, S, and $\tilde{W}$ are uniformly ultimately semi-global bounded in a compact set dgnals of the horizontal position subsystem are semi-globally finite-time stable in a compact set $\Omega_{q_2} \equiv \{q_2 : \|q_2\| \le c_{q_2}\}$.

Theorem 3: For the horizontal position subsystem (33), if the FTSM surface is set as (35), the control input and the adaptive law are designed as (43) and (44) respectively, then all the closed loop signals of the horizontal position subsystem are semi-globally finite-time stable in a compact set $\Omega_{q_2} \equiv \{q_2 : \|q_2\| \le c_{q_2}\}$.

IV. Simulation

In this part, the performance and the superiority of the proposed control methodology is demonstrated in the presence of parametric uncertainties, unknown functions, and unknown external disturbances. For the sake of comparison, we consider the robust integral of the signum error (RISE) [37], RBFNN based proportional-derivative SMC (NN-PD-SMC) [37], adaptive back-stepping with fast terminal SMC (ABFTSMC) [48] and fractional order SMC (FSMC) [9]

For the quadrotor parameters, refer to [47]. The NNFISMC parameters are $\lambda_1 = 20 \times \text{diag}\{1,1,1,1\}, \Lambda = 24 \times \text{diag}\{1,1,1,1\}$, $\eta = 20 \times \text{diag}\{1,1,1,1\}$, $c = \text{diag}\{2,2,2.5,6\}$, $K = \text{diag}\{4.5,4.5,4.5,6\}$. The order of the fractional derivative is $\sigma = 0.2$. The RBFNN tuning parameters are $\xi_1 = 10^{-3} \times \text{diag}\{1.5,1.5,1.5,1.5\}$, $\xi_2 = 10^{-3} \times \text{diag}\{2,2,2,2\}$. The parameters of NN-BFTSMS are $c = \text{diag}\{20,20\}, h = 2 \times 10^{-3}\text{diag}\{1,1\}, K = \text{diag}\{24,24\}, \xi_3 = \text{diag}\{0.15,0.15\}$ $\mu = 0.001, \gamma_j = 1$ and

$$c_j = \begin{bmatrix} -0.5 & -0.25 & 0 & 0.25 & 0.5 \\ -0.5 & -0.25 & 0 & 0.25 & 0.5 \end{bmatrix}.$$

The desired trajectories are given by

$$\Upsilon_d = \begin{bmatrix} \sin(0.8t) \\ \arcsin\left(u_x \sin\psi - u_y \cos\psi\right) \\ \arcsin\left(\frac{u_x \cos\psi + u_y \sin\psi}{\cos\phi_d}\right) \\ 0.5\sin(0.5t) \end{bmatrix}; \; M_d = \begin{bmatrix} 2 \\ 1 \end{bmatrix}.$$

A parametric uncertainty $\Delta = 40\%$ is considered and the sinusoidal external disturbances are given by

$$\delta_1 = \begin{bmatrix} 5\cos(4t) \\ 5\sin(4t)\cos(3t) \\ 5\sin(4t) \\ 5(\cos(5t) + \sin(2t)) \end{bmatrix}; \delta_2 = \begin{bmatrix} 3(\cos(0.5t) + \sin(2t)) \\ 2\cos(0.5t)\sin(0.5t) \end{bmatrix}.$$

The simulation results are depicted in Figs. 2-6. The responses of the quadrotor fully-actuated subsystem are shown in 2. It is clear that under the action of both FSMC and RISE, the pitch and roll angles failed to stabilized to zero while the yaw angle and the vertical position settle very close to the desired trajectories. It is worth noting that FSMC in [9] and RISE in [37] provided excellent tracking result in the presence of the small amplitude sinusoidal disturbances. Nonetheless, in this work, the controllers performed poorly in the presence of sinusoidal disturbances with bigger amplitudes. The poor performances are due to the fact that the controllers lack online estimation algorithm to estimate and overcome the time varying disturbances. By contrast, the NN-FISMC derives the fully-actuated subsystem to follow the desired trajectories in finite time. This is because NN-FISMC integrates the approximation ability of RBFNN to learn the uncertain functions and high amplitude disturbances, the fractional order derivative of the tracking error for improved robustness, and the integral error action to eliminate the steady state errors. As presented in Fig. 3, the NN-FISMC is able to achieve null steady state errors unlike the FSMC and RISE.

The horizontal position tracking responses are depicted in Fig. 4. It can be seen that the horizontal position coordinates trace the desired signals under the ABFTSMC due to its ability to estimate and compensate the upper-bound of the disturbances. The NN-PD-SMC gives an improved performances with lower rise and settling times compared to the ABFTSM. The NN incorporated to the PD-SMC identifies the time varying disturbances thereby providing better disturbance suppression than ABFTSMC. Replacing the adaptation mechanism of ABFTSMC with RBFNN results in the proposed NNBFTSMC. It is clear that the performance of the NN-BFTSMC is superior to that of both NN-PD-SMC and ABFTSMC in terms of the rise and the settling times. Furthermore, the tracking errors of the horizontal position converge to zero

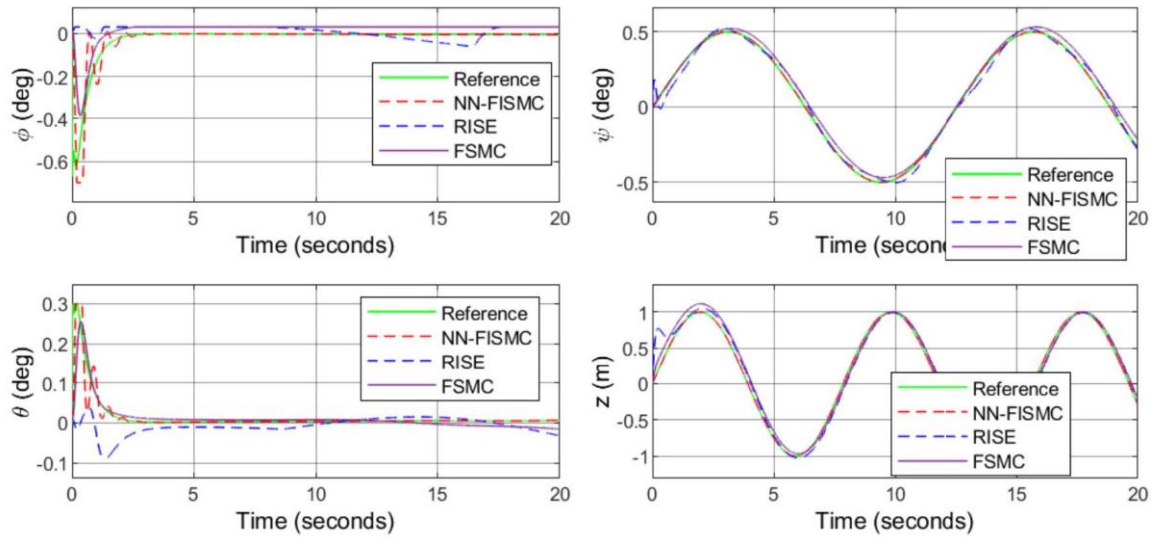

Fig. 2. Attitude tracking

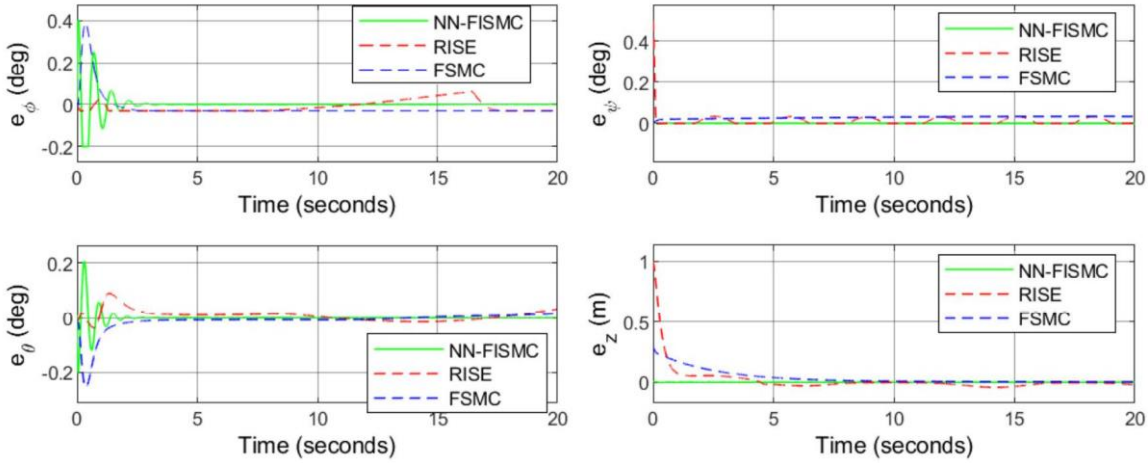

Fig. 3. Attitude tracking errors

faster with NN-BFTSMC than with both ABFTSMC and NNPD-SMC as shown in Fig. 5. The control inputs are displayed in Fig. 6.

V. Conclusions

In this article, a robust finite time NN-FISMC and NNBFTSMC are developed to tackle the trajectory tracking issue of a quadrotor suffering from external disturbances and uncertainties. First and foremost, a NN-FISMC has been designed for the fully-actuated subsystem. Furthermore, a NN-BFTSMC has been designed to control the under-actuated subsystem and generate the desired pitch and roll angles. Simulation results have shown that the robust hierarchical control structure, NN-FSMC combine with NN-BFTSMC, ensures excellent attenuation of external disturbances and convergence of the quadrotor trajectories to the desired states in a short time. The closed loop system has been proved to converge to a small compact set near the origin in finite time. Future work will further validate the efficacy of the proposed controller on a real-time quadrotor.

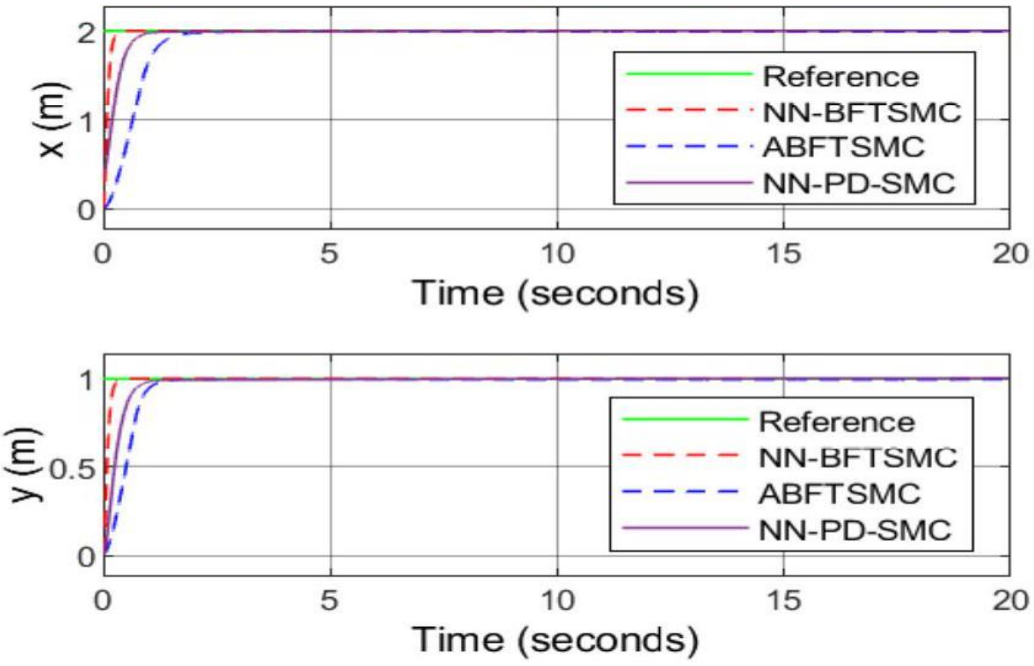

Fig. 4. Position tracking

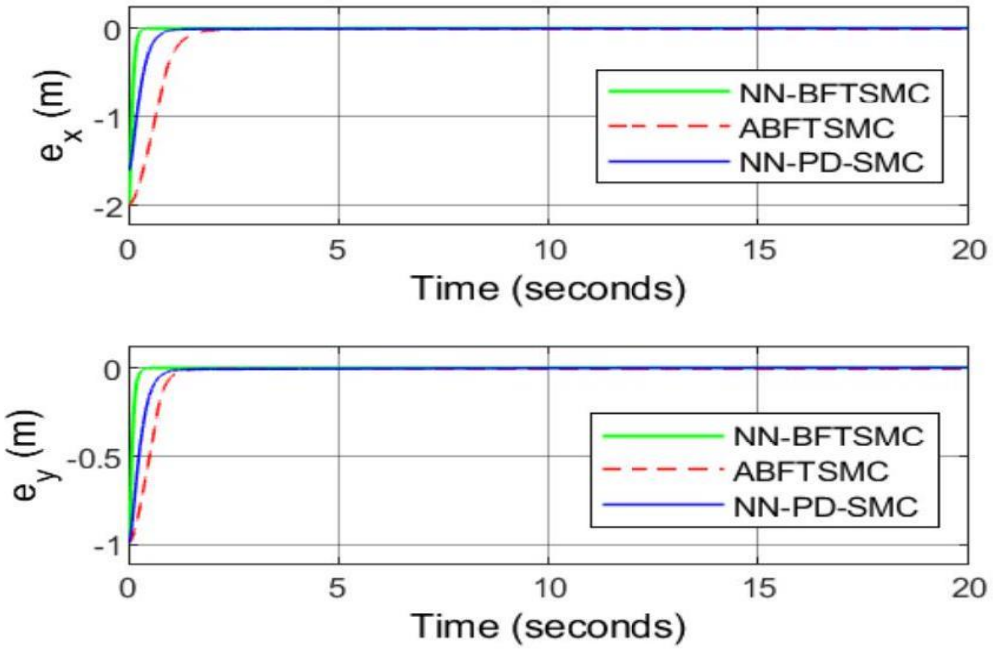

Fig. 5. Position tracking errors

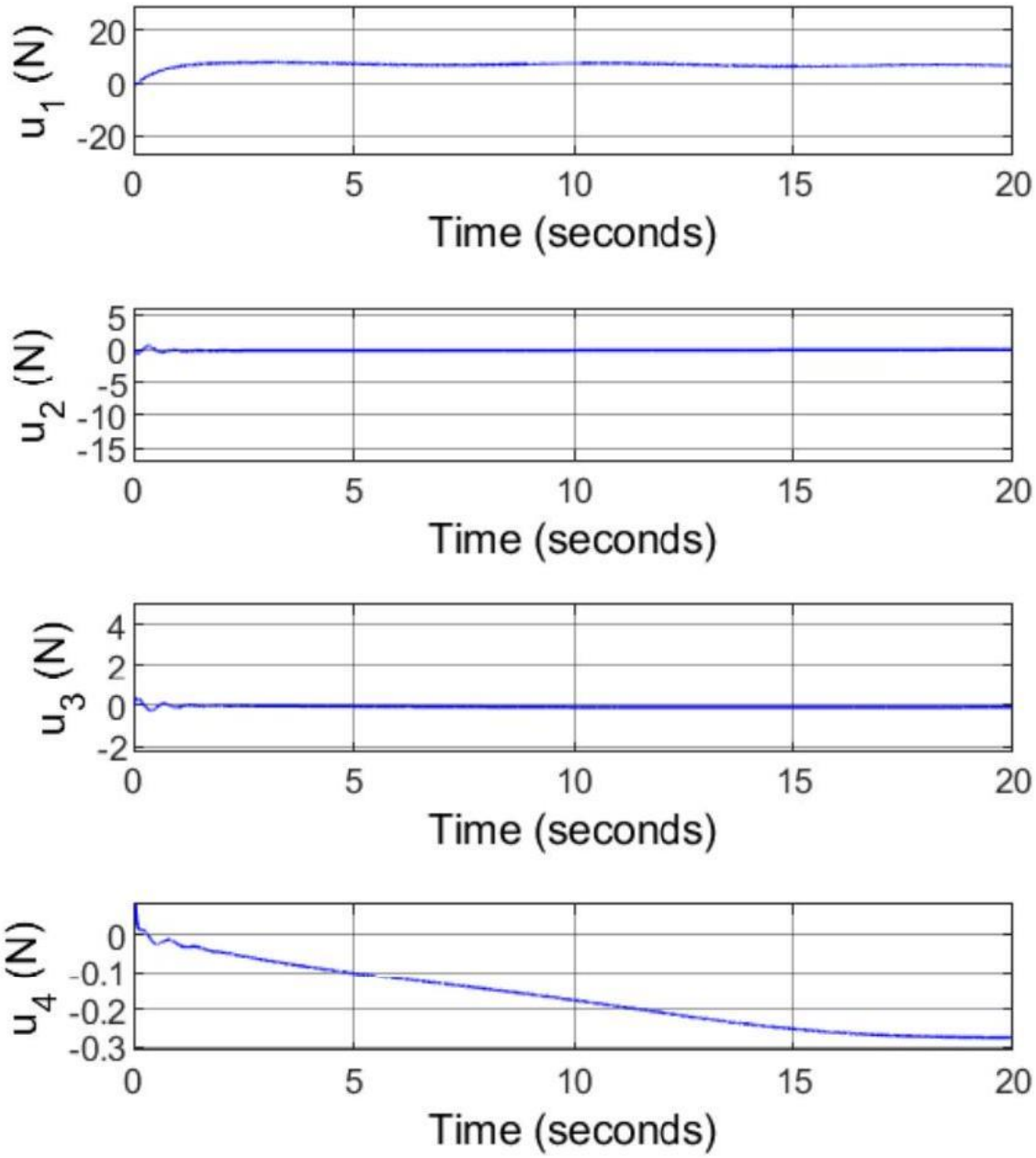

Fig. 6. Control inputs

REFERENCES

1. H. Razmi and S. Afshinfar, "Neural network-based adaptive sliding mode control design for position and attitude control of a quadrotor uav," Aerospace Science and Technology, vol. 91, pp. 12 - 27, 2019.
2. M. S. Mahmoud and M. Maaruf, "Robust adaptive multilevel control of a quadrotor," IEEE Access, vol. 8, pp. 167 684-167 692, 2020.
3. W. Wang and X. Yu, "Chattering free and nonsingular terminal sliding mode control for attitude tracking of a quadrotor," in 2017 29th Chinese Control and Decision Conference (CCDC), May 2017, pp. 719-723.
4. M. Labbadi and M. Cherkaoui, "Robust adaptive nonsingular fast terminal sliding-mode tracking control for an uncertain quadrotor uav subjected to disturbances," ISA Transactions, 2019.
5. M. Maaruf, A. Babangida, H. A. Almusawi, and P. S. Tamas, "Neural network-based finite-time control of nonlinear systems with unknown dead-zones: Application to quadrotors," Journal of Robotics and Control (JRC), vol. 3, no. 6, pp. 735-742, 2022.
6. M. Vahdanipour and M. Khodabandeh, "Adaptive fractional order sliding mode control for a quadrotor with a varying load," Aerospace Science and Technology, vol. 86, pp. 737 – 747,2019.

7. C. Hua, J. Chen, and X. Guan, "Fractional-order sliding mode control of uncertain quavs with time-varying state constraints," Nonlinear Dynamics, vol. 95, no. 2, pp. 1347-1360, Jan 2019.
8. H. L. Maurya, A. K. Kamath, N. K. Verma, and L. Behera, "Vision-based fractional order sliding mode control for autonomous vehicle tracking by a quadrotor uav," in 2019 28th IEEE International Conference on Robot and Human Interactive Communication (RO-MAN), 2019, pp. 1-6.
9. M. Labbadi, S. Nassiri, L. Bousselamti, M. Bahij, and M. Cherkaoui, "Fractional-order fast terminal sliding mode control of uncertain quadrotor uav with time-varying disturbances," in 2019 8th International Conference on Systems and Control (ICSC), 2019, pp. 417-422.
10. X. Wu, B. Xiao, and Y. Qu, "Modeling and sliding mode-based attitude tracking control of a quadrotor uav with time-varying mass," ISA Transactions, 2019.
11. M. Kahouadji, M. R. Mokhtari, A. Choukchou-Braham, and B. Cherki, "Real-time attitude control of 3 dof quadrotor uav using modified supe twisting algorithm," Journal of the Franklin Institute, 2019.
12. W. Cai, J. She, M. Wu, and Y. Ohyama, "Disturbance suppression for quadrotor uav using sliding-mode-observer-based equivalent-inputdisturbance approach," ISA Transactions, vol. 92, pp. 286 - 297, 2019.
13. X. Wang, S. Sun, E.-J. van Kampen, and Q. Chu, "Quadrotor fault tolerant incremental sliding mode control driven by sliding mode disturbance observers," Aerospace Science and Technology, vol. 87, pp. 417 – 430 2019.
14. M. Chen, S. Xiong, and Q. Wu, "Tracking flight control of quadrotor based on disturbance observer," IEEE Transactions on Systems, Man, and Cybernetics: Systems, pp. 1-10, 2019.
15. "Tracking flight control of quadrotor based on disturbance observer," IEEE Transactions on Systems, Man, and Cybernetics: Systems, pp. 1-10, 2019.
16. J. Zheng and P. Li, "Fault tolerant control of actuator additive fault for quadrotor based on sliding mode observer," in 2019 Chinese Control and Decision Conference (CCDC), June 2019, pp. 5908-5913.
17. B. Wang, X. Yu, L. Mu, and Y. Zhang, "Disturbance observer-based adaptive fault-tolerant control for a quadrotor helicopter subject to parametric uncertainties and external disturbances," Mechanical Systems and Signal Processing, vol. 120, pp. 727 - 743, 2019.
18. Z. Liu, C. Yuan, X. Yu, and Y. Zhang, "Retrofit fault-tolerant tracking control design of an unmanned quadrotor helicopter considering actuato dynamics," International Journal of Robust and Nonlinear Control, vol. 29, no. 16, pp. 5293-5313, 2019.
19. D. Ma, Y. Xia, G. Shen, Z. Jia, and T. Li, "Flatness-based adaptive sliding mode tracking control for a quadrotor with disturbances," Journal of the Franklin Institute, vol. 355, no. 14, pp. 6300 - 6322, 2018.
20. R. Miranda-Colorado and L. T. Aguilar, "Robust pid control of quadrotors with power reduction analysis," ISA Transactions, 2019.
21. K. Zhao, J. Zhang, D. Ma, and Y. Xia, "Composite disturbance rejection attitude control for quadrotor with unknown disturbance," IEEE Transactions on Industrial Electronics, pp. 1-1, 2019.
22. L. Zhao, L. Dai, Y. Xia, and P. Li, "Attitude control for quadrotors subjected to wind disturbances via active disturbance rejection control and integral sliding mode control," Mechanical Systems and Signal Processing, vol. 129, pp. 531 – 545,2019.
23. Z. Cai, J. Lou, J. Zhao, K. Wu, N. Liu, and Y. X. Wang, "Quadrotor trajectory tracking and obstacle avoidance by chaotic grey wolf optimization-based active disturbance rejection control," Mechanical Systems and Signal Processing, vol. 128, pp. 636 - 654, 2019.
24. Y. Zhang, Z. Chen, X. Zhang, Q. Sun, and M. Sun, "A novel control scheme for quadrotor uav based upon active disturbance rejection control," Aerospace Science and Technology, vol. 79, pp. 601 - 609 2018.
25. Hao Liu, Wanbing Zhao, Sheng Hong, Frank L. Lewis, and Yao Yu, "Robust backstepping-based trajectory tracking control for quadrotors with time delays," IET Control Theory & Applications, vol. 13, pp 1945-1954(9), August 2019.
26. D. Cabecinhas, R. Cunha, and C. Silvestre, "A trajectory tracking control law for a quadrotor with slung load," Automatica, vol. 106, pp. 384 – 389,2019.
27. J. Zeng and K. Sreenath, "Geometric control of a quadrotor with a load suspended from an offset," in 2019 American Control Conference (ACC), 2019, pp. 3044-3050.
28. N. Liu, X. Shao, J. Li, and W. Zhang, "Attitude restricted back-stepping anti-disturbance control for vision-based quadrotors with visibility constraint," ISA Transactions, 2019.
29. A. Noormohammadi-Asl, O. Esrafilian, M. A. Arzati, and H. D. Taghirad, "System identification and h_∞-based control of quadrotor attitude," Mechanical Systems and Signal Processing, vol. 135, p. 106358, 2020.
30. X. Shao, J. Liu, and H. Wang, "Robust back-stepping output feedback trajectory tracking for quadrotors via extended state observer and sigmoid tracking differentiator," Mechanical Systems and Signal Processing, vol. 104, pp. 631 - 647, 2018.
31. Y. Wang and K. Cao, "Integral terminal sliding mode-based flight control for quadrotor uavs," in 2019 Eleventh International Conference on Advanced Computational Intelligence (ICACI), June 2019, pp. 78-83.
32. H. Bouadi and F. Mora-Camino, "Modeling and adaptive flight control for quadrotor trajectory tracking," Journal of Aircraft, vol. 55, no. 2, pp 666-681, 2018

33. M. E. Antonio-Toledo, E. N. Sanchez, A. Y. Alanis, J. Flórez, and M. A. Perez-Cisneros, "Real-time integral backstepping with sliding mode control for a quadrotor uav," IFAC-PapersOnLine, vol. 51, no. 13, pp. 549 - 554, 2018, 2nd IFAC Conference on Modelling, Identification and Control of Nonlinear Systems MICNON 2018.
34. M. He and J. He, "Extended state observer-based robust backstepping sliding mode control for a small-size helicopter," IEEE Access, vol. 6, pp. 33480 – 33488,2018
35. M. Maaruf, W. M. Hamanah, and M. A. Abido, "Hybrid backstepping control of a quadrotor using a radial basis function neural network," Mathematics, vol. 11, no. 4, p. 991, 2023.
36. X. Shao, N. Liu, Z. Wang, W. Zhang, and W. Yang, "Neuroadaptive integral robust control of visual quadrotor for tracking a moving object," Mechanical Systems and Signal Processing, vol. 136, p. 106513, 2020.
37. Z. Li, X. Ma, and Y. Li, "Robust tracking control strategy for a quadrotor using rpd-smc and rise," Neurocomputing, vol. 331, pp. 312 - 322, 2019
38. W. K. Alqaisi, B. Brahmi, J. Ghommam, M. Saad, and V. Nerguizian, "Adaptive sliding mode control based on rbf neural network approximation for quadrotor," in 2019 IEEE International Symposium on Robotic and Sensors Environments (ROSE), 2019, pp. 1-7.
39. X. Shi, Y. Cheng, C. Yin, H. Shi, and X. Huang, "Actuator fault tolerant controlling using adaptive radical basis function neural network smc for quadrotor uav," in 2019 Chinese Control and Decision Conference (CCDC), 2019, pp. 5409-5414.
40. T. Abdollahi, S. Salehfard, and J.-F. Y. Cai-Hua Xiong, "Simplified fuzzy-padé controller for attitude control of quadrotor helicopters," IET Control Theory & Applications, vol. 12, pp. 310-317(7), January 2018
41. T.-L. Liao, W.-S. Chan, and J.-J. Yan, "Distributed adaptive dynamic surface formation control for uncertain multiple quadrotor systems with interval type-2 fuzzy neural networks," Transactions of the Institute of Measurement and Control, vol. 41, no. 7, pp. 1861-1879, 2019.
42. X. Yu, Z. Lv, Y. Wu, and X. Sun, "Neural network modeling and backstepping control for quadrotor," in 2018 Chinese Automation Congress (CAC), Nov 2018, pp. 3649-3654.
43. S. Li, Y. Wang, J. Tan, and Y. Zheng, "Adaptive rbfnns/integral sliding mode control for a quadrotor aircraft," Neurocomputing, vol. 216, pp. 126 - 134, 2016. [Online]. Available: http://www.sciencedirect.com/ science/article/pii/S0925231216307780
44. J. Zhou, Y. Cheng, H. Du, D. Wu, M. Zhu, and X. Lin, "Active finitetime disturbance rejection control for attitude tracking of quad-rotor under input saturation," Journal of the Franklin Institute, 2019.
45. N. Wang, Q. Deng, G. Xie, and X. Pan, "Hybrid finite-time trajectory tracking control of a quadrotor," ISA Transactions, vol. 90, pp. 278 – 286, 2019.
46. B. Tian, J. Cui, H. Lu, Z. Zuo, and Q. Zong, "Adaptive finite-time attitude tracking of quadrotors with experiments and comparisons," IEEE Transactions on Industrial Electronics, vol. 66, no. 12, pp. 9428-9438, Dec 2019
47. O. Mofid and S. Mobayen, "Adaptive sliding mode control for finitetime stability of quad-rotor uavs with parametric uncertainties," ISA Transactions, vol. 72, pp. 1 – 14,2018.
48. M. Labbadi and M. Cherkaoui, "Robust adaptive backstepping fast terminal sliding mode controller for uncertain quadrotor uav," Aerospace Science and Technology, vol. 93, p. 105306, 2019.
49. M. Maaruf, M. S. Mahmoud, and A. Ma'arif, "A survey of control methods for quadrotor uav," International Journal of Robotics and Control Systems, vol. 2, no. 4, pp. 652-665, 2022
50. H. Wang, "Adaptive finite-time control for a class of uncertain high order non-linear systems based on fuzzy approximation," IET Control Theory & Applications, vol. 11, pp. 677-684(7), March 2017
51. M. Maaruf and M. Khalid, "Global sliding-mode control with fractionalorder terms for the robust optimal operation of a hybrid renewable microgrid with battery energy storage," Electronics, vol. 11, no. 1, p. 88 2021.
52. F. L. Lewis, A. Yesildirak, and S. Jagannathan, Neural Network Control of Robot Manipulators and Nonlinear Systems. Bristol, PA, USA: Taylor & Francis, Inc., 1998
53. H. C., C. J., and G. X., "Fractional-order sliding mode control of uncertain quavs with time-varying state constraints," Nonlinear Dyn, vol. 95, pp. 1347 - 1360, 2019.

CITATION
Abdussamad M.F, Abubakar S.I, Lawal M.I, Mukhtar I.B, & Muhammad A.B. (2024). Adaptive Control of Quadrotor with Neural disturbance Estimator. In Global Journal of Research in Engineering & Computer Sciences (Vol. 4, Number 4, pp. 88–101). https://doi.org/10.5281/zenodo.13175683